Numerical mass balance for soil-moisture transport problems

T. V. HROMADKA II and G. L. GUYMON
School of Engineering, University of California, Irvine, CA, 92717, USA

The Galerkin finite element method coupled with the Crank–Nicolson time advance procedure is often used as a numerical analog for unsaturated soil-moisture transport problems. The Crank–Nicolson procedure leads to numerical mass balance problems which results in instability. A new temporal and spatial integration procedure is proposed that exactly satisfies mass balance for the approximating function used. This is accomplished by fitting polynomials continuously throughout the time and space domain and integrating the governing differential equations. To reduce computational effort, the resulting higher order polynomials are reduced to quadratic and linear piece-wise continuous polynomial approximation functions analogous to the finite element approach. Results indicate a substantial improvement in accuracy over the combined Galerkin and Crank–Nicolson methods when comparing to simplified problems where analytical solutions are available.

INTRODUCTION

Finite element techniques have been applied to numerical solutions of moisture transfer in soils by a number of investigators[1,7]. A substantial amount of work has been done on the efficiency and accuracy of finite element Galerkin techniques[3,5,8]. In the case of moisture transfer in unsaturated soils, the equation of state is non-linear and generally in order to apply the finite element method the governing differential equation of state is linearized by forcing parameters to be constant within each finite element. Hromadka and Guymon[6] investigate the numerical effects of various approximations for determining the constant parameters, but assume that the time derivative term is approximated by the Crank–Nicolson time advancement routine. In this paper the coupled numerical analogs based upon the Galerkin finite element method and Crank–Nicolson method are examined in respect to satisfaction of mass balance in the governing equation of state. A numerical modification to the finite element analog of moisture transfer in a horizontal soil column is presented, and extensions to moisture transfer in a vertical soil column and a two-dimensional soil system are included.

TRANSPORT ANALOG

Horizontal infiltration of water into a homogeneous soil column of length L having an initial water content θ_0 and suddenly subjected for time $t>0$ to a greater constant water content θ_1 at $x=0$ is described by:

$$\frac{\partial}{\partial x}\left[D(\theta)\frac{\partial\theta}{\partial x}\right]=\frac{\partial\theta}{\partial t} \tag{1}$$

$$\theta=\theta_0 \quad t=0 \quad 0\leqslant x\leqslant L$$

$$\theta=\theta_1 \quad t>0 \quad x=0 \tag{2}$$

where θ is the dimensionless soil volumetric water content; x is the horizontal spatial coordinate; t is time; and $D(\theta)$ is the soil water diffusivity.

The finite element approach used to solve equations (1) and (2) is the Galerkin version of the weighted residual process[2]. The solution domain is discretized into the union of n finite elements by:

$$L=\bigcup_{i=1}^{n} L_i \tag{3}$$

The water content is utilized as the state variable and is approximated within each finite element by:

$$\theta(x,t)=\sum N_j(x,t)\theta_j \tag{4}$$

where N_j is the appropriate linearly independent shape functions; θ_j is the state variable values at elemental-nodal points designated by the general summation index j.

The Galerkin technique utilizes the set of shape functions as the weighting functions, which indicates that the corresponding finite element representation for the infiltration process is

$$\int\left\{\frac{\partial}{\partial x}\left[D(\theta)\frac{\partial\theta}{\partial x}\right]-\frac{\partial\theta}{\partial t}\right\}N_j\,dx=0 \tag{5}$$

Integration by parts expands equation (5) into the form:

$$\sum_{i=1}^{n}\left\{D(\theta)\frac{\partial\theta}{\partial x}N_j\Big|_{S_i}-\int_{L_i}\left[D(\theta)\frac{\partial\theta}{\partial x}\frac{\partial N_j}{\partial x}+N_j\frac{\partial\theta}{\partial t}\right]dx\right\}=0 \tag{6}$$

where S_i is the external endpoints of the one-dimensional finite element, L_i. The first term within the braces negates to zero for interior elements and also satisfies the usual

0309-1708/80/030107-08$02.00

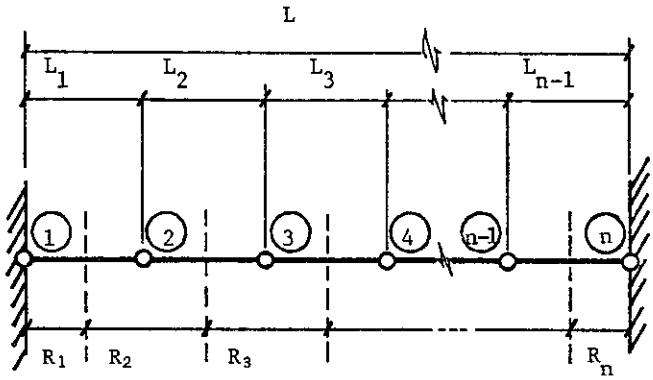

Figure 1. One-dimensional nodal domain. (1) *= nodal point number 1;* R_1 *= nodal domain number 1;* L *~ column length*

specified (or flux type) boundary conditions of the problem for exterior finite elements. The remaining integral term is solved by substituting the appropriate element approximations and shape functions into the integrand and solving by numerical integration. The non-linear nature of the partial differential equation, however, generally introduces difficulties in integrating equation (6). It is customary to deal with this problem by assuming the diffusivity function to be constant within each finite element during a finite time interval, Δt (e.g. Guymon and Luthin[4]). The Crank–Nicolson time advancement approximation has been widely used[2,5] to solve the time derivation of equation (6). The time derivative could also be approximated by the Galerkin technique[1]; however, it does not appear to be advantageous[9].

The Crank–Nicolson formulation reduces equation (6), where values of soil-water diffusivity are assumed constant within each finite element, into a system of linear equations expressed in matrix form as:

$$\left\{\mathbf{P}+\frac{\Delta t}{2}\mathbf{S}\right\}\theta^{i+1}=\left\{\mathbf{P}-\frac{\Delta t}{2}\mathbf{S}\right\}\theta^{i} \tag{7}$$

where **P** is a symmetrical capacitance matrix and is a function of element nodal global coordinates; **S** is a symmetrical stiffness matrix and is a function of element nodal global coordinates and constant finite element diffusivity coefficients (during time step Δt); Δt is the finite time step increment; and θ^k is the vector of nodal state variable approximations (volumetric water content) at time steps $k=i, i+1$.

Hromadka and Guymon[6] show that the numerical expressions of the combined equations (6) and (7) results in an incorrect balance of mass for each nodal solution. To correct the mass-balance relations, the time-integrated influx of moisture was equated to the net integrated spatial variation of moisture content. For the special case of a Galerkin linear shape-function approximation (with the Crank–Nicolson time advancement procedure), a modified finite element capacitance matrix was developed; however, a detailed mathematical analysis of the matrix modification was not presented. The following discussion addresses the mathematical development of the modified finite element capacitance matrix (for solution of equation (1)) and extends the modifications to include the so-called convection–diffusion class of equations (i.e., a vertical soil column problem), and finally develops a two-dimensional horizontal moisture transport analog.

MATHEMATICAL DEVELOPMENT

Assume the soil column is discretized into n disjoint domains by n nodal points as shown in Fig. 1 where:

$$\left.\begin{aligned} R_1 &\equiv \left\{x \mid 0 \leqslant x \leqslant \frac{L_1}{2}\right\} \\ R_j &\equiv \left\{x \mid x(\theta_j)-\frac{L_{j-1}}{2} < x \leqslant x(\theta_j)+\frac{L_j}{2}\right\} \\ R_n &\equiv \left\{x \mid x(\theta_n)-\frac{L_{n-1}}{2} < x \leqslant L\right\} \\ R &\equiv \bigcup_{j=1}^{n} R_j \end{aligned}\right\} \tag{8}$$

where θ_j is the value of state variable at spatial increment j and L_j is the redefined spatial length between nodal points (θ_j, θ_{j+1}).

The solution of equation (1) within each nodal domain determines n equations:

$$\left.\begin{aligned} &\frac{\partial}{\partial x}\left[D(\theta)\frac{\partial\theta}{\partial x}\right]=\frac{\partial\theta}{\partial t};\ x\in R_1 \\ &\frac{\partial}{\partial x}\left[D(\theta)\frac{\partial\theta}{\partial x}\right]=\frac{\partial\theta}{\partial t};\ x\in R_2 \\ &\qquad\vdots \\ &\frac{\partial}{\partial x}\left[D(\theta)\frac{\partial\theta}{\partial x}\right]=\frac{\partial\theta}{\partial t};\ x\in R_n \end{aligned}\right\} \tag{9}$$

Using a local coordinate system defined by:

$$\left.\begin{aligned} &\frac{dy}{dx}=1 \\ &R_j \equiv \{y \mid 0 < y < l_j\} \end{aligned}\right\} \tag{10}$$

the system defined by equations in (9) can be integrated to give:

$$\begin{bmatrix} \int_{\Delta t}\int_{R_1}\frac{\partial}{\partial y}\left[D(\theta)\frac{\partial\theta}{\partial y}\right]dy\,dt \\ \int_{\Delta t}\int_{R_2}\frac{\partial}{\partial y}\left[D(\theta)\frac{\partial\theta}{\partial y}\right]dy\,dt \\ \vdots \\ \int_{\Delta t}\int_{R_n}\frac{\partial}{\partial y}\left[D(\theta)\frac{\partial\theta}{\partial y}\right]dy\,dt \end{bmatrix} = \begin{bmatrix} \int_{\Delta t}\int_{R_1}\frac{\partial\theta}{\partial t}\,dy\,dt \\ \int_{\Delta t}\int_{R_2}\frac{\partial\theta}{\partial t}\,dy\,dt \\ \vdots \\ \int_{\Delta t}\int_{R_n}\frac{\partial\theta}{\partial t}\,dy\,dt \end{bmatrix} \tag{11}$$

where the temporal integration is assumed to occur over a time-step increment of Δt. Equation (11) can be rewritten as:

$$\begin{bmatrix} \int_{k\Delta t}^{(k+1)\Delta t} \left\{ D \frac{\partial \theta}{\partial y} \Big|_{0}^{l_1} \right\} dt \\ \int_{k\Delta t}^{(k+1)\Delta t} \left\{ D \frac{\partial \theta}{\partial y} \Big|_{0}^{l_2} \right\} dt \\ \vdots \\ \int_{k\Delta t}^{(k+1)\Delta t} \left\{ D \frac{\partial \theta}{\partial y} \Big|_{0}^{l_n} \right\} dt \end{bmatrix} = \begin{bmatrix} \int_{0}^{l_1} \left\{ \theta \Big|_{k\Delta t}^{(k+1)\Delta t} \right\} dy \\ \int_{0}^{l_2} \left\{ \theta \Big|_{k\Delta t}^{(k+1)\Delta t} \right\} dy \\ \vdots \\ \int_{0}^{l_n} \left\{ \theta \Big|_{k\Delta t}^{(k+1)\Delta t} \right\} dy \end{bmatrix} \tag{12}$$

where k is the temporal time step increment.

The state variable, θ, can be approximated spatially throughout R by the Ritz formulation; i.e.

$$\hat{\theta}(x, t_0) = \sum_{j=1}^{n} N_j(x)\theta_j \tag{13}$$

where N_j is the appropriate polynomial spatial shape function and θ_j is the state variable value at nodal points designated by the general summation index j. Additionally, let θ be approximated temporally by:

$$\theta^*(x_0, t) = \sum_{m=-1}^{k+1} M_m \theta^m \tag{14}$$

where M_m is the appropriate polynomial temporal shape function and θ^m is the state variable value at nodal points designated by the general summation index m; $m=0$ indicates the initial condition, $m=-1$ indicates the condition at time step $(-\Delta t)$.

Equations (13) and (14) can be combined as:

$$\left.\begin{aligned} \hat{\theta}(x, t) &= \sum_{j=1}^{n} N_j(x)\theta_j^* \\ \theta_j^* &= \sum_{m=-1}^{k+1} M_m \theta^m \end{aligned}\right\} \tag{15}$$

where the θ_n^m are known values of the state variable for time steps $(-1, 0, 1, \ldots, k)$.

Combining equations (12) and (15) yields:

$$\begin{bmatrix} \int_{k\Delta t}^{(k+1)\Delta t} \left\{ D \frac{\partial \hat{\theta}}{\partial y} \Big|_{0}^{l_1} \right\} dt \\ \int_{k\Delta t}^{(k+1)\Delta t} \left\{ D \frac{\partial \hat{\theta}}{\partial y} \Big|_{0}^{l_2} \right\} dt \\ \vdots \\ \int_{k\Delta t}^{(k+1)\Delta t} \left\{ D \frac{\partial \hat{\theta}}{\partial y} \Big|_{0}^{l_n} \right\} dt \end{bmatrix}_C = \begin{bmatrix} \int_{0}^{l_1} \left\{ \hat{\theta} \Big|_{k\Delta t}^{(k+1)\Delta t} \right\} dy \\ \int_{0}^{l_2} \left\{ \hat{\theta} \Big|_{k\Delta t}^{(k+1)\Delta t} \right\} dy \\ \vdots \\ \int_{0}^{l_n} \left\{ \hat{\theta} \Big|_{k\Delta t}^{(k+1)\Delta t} \right\} dy \end{bmatrix} \tag{16}$$

The solution of equation (16) where water content is approximated by equation (15) results in increasing computational effort as the time solution progresses. By approximating water content both spatially and temporally by sets of piecewise continuous polynomials, the numerical effort is considerably reduced.

For discussion purposes, let the l_j be uniform throughout R, and soil-water diffusivity held constant during time step Δt,

$$\left.\begin{aligned} &l_i = \Delta x;\ i = 1, 2, \ldots, n \\ &l_1 = l_n = \Delta x/2 \\ &\frac{\partial D}{\partial t} = 0;\ k\Delta t < t < (k+1)\Delta t \end{aligned}\right\} \tag{17}$$

Then for water content characterized by parabolas both spatially and temporally:

$$\left.\begin{aligned} \hat{\theta}(y, t_0) &= \left[\frac{\theta_0 - 2\theta_1 + \theta_2}{2(\Delta x)^2}\right] y^2 + \left[\frac{4\theta_1 - 3\theta_0 - \theta_2}{2\Delta x}\right] y + \theta_0 \\ \hat{\theta}(y_0, t) &= \left[\frac{\theta^0 - 2\theta^1 + \theta^2}{2(\Delta t)^2}\right] t^2 + \left[\frac{4\theta^1 - 3\theta^0 - \theta^2}{2\Delta x}\right] t + \theta^0 \end{aligned}\right\} \tag{18}$$

where $(\theta_0, \theta_1, \theta_2)$ represent typical nodal points separated by the constant spatial increment Δx; and $(\theta^0, \theta^1, \theta^2)$ represent typical nodal points separated by the constant temporal increment Δt. The spatial gradient of water content is evaluated by:

$$\left.\begin{aligned} \frac{\partial \theta}{\partial y}\Big|_0 &= (\theta_1^* - \theta_0^*)/\Delta x \\ \frac{\partial \theta}{\partial y}\Big|^{\Delta x} &= (\theta_2^* - \theta_1^*)/\Delta x \\ \theta\left(y = \frac{\Delta x}{2}\right) &= \theta_1^* \end{aligned}\right\} \tag{19}$$

where the starred terms represent functions of time as defined by equation (18). In order to coincide interpolating parabolas between nodal points, the average of all interpolating parabolas within a nodal domain are used. Accordingly, interior nodal points may have up to five nodal points contributing to each nodal point's numerical solution.

NUMERICAL MODEL VERIFICATION

The proposed numerical scheme was applied to the normalized soil moisture transfer problem:

$$\frac{\partial^2 \theta}{\partial x^2} = \frac{\partial \theta}{\partial t} \qquad 0 \leqslant x \leqslant 1 \tag{20}$$

with boundary conditions

$$\theta(0, t) = (1, t) = 0 \qquad t > 0 \tag{21}$$

and initial condition

$$\theta(x, 0)=1 \tag{22}$$

The exact solution is the well-known series expansion:

$$\theta(x, t)=\frac{4}{\pi}(\sin \pi x e^{-\pi^2 t}+\frac{\sin 3\pi x}{3} e^{-9\pi^2 t}+\ldots) \tag{23}$$

For the normalized soil moisture transfer problem, the numerical approach of equations (16) and (18) reduces to the following set of linear equations:

$$\frac{\Delta t}{12(\Delta x)}\{-(\theta_1^0-2\theta_2^0+3\theta_3^0)+8(\theta_1^1-2\theta_2^1+\theta_3^1)+$$

$$5(\theta_1^2-2\theta_2^2+\theta_3^2)\}=\frac{\Delta x}{48}\{-(\theta_0^2+6\theta_1^2+38\theta_2^2+6\theta_3^2-\theta_4^2)-$$

$$(-\theta_0^1+6\theta_1^1+38\theta_2^1+6\theta_3^1-\theta_4^1)\} \tag{24}$$

The first set of braces equals the net integrated influx of moisture between time steps Δt and $2\Delta t$ (superscripts 1 and 2, respectively); the second set of braces is the integrated variation of water content during the time advancement. For $\beta=4(\Delta t)/(\Delta x)^2$, equation (24) may be rewritten as:

$$-\theta_0^2+\theta_1^2(6-5\beta)+\theta_2^2(38+10\beta)+\theta_3^2(6-5\beta)-\theta_4^2$$

$$=-\beta(\theta_1^0-2\theta_2^0+\theta_3^0)+\theta_1^1(6+8\beta)+\theta_2^1(38-16\beta)+$$

$$\theta_3^1(6+8\beta)-(\theta_0^1+\theta_4^1) \tag{25}$$

where superscripts and subscripts refer to temporal and spatial coordinates. Appropriate integration with respect to space and time on column-end nodal domains gives for the global matrix system (with specified boundary conditions)

$$\begin{bmatrix} 1 & 0 & 0 & 0 & \cdots & \cdots & \cdots & 0 \\ (3-5\beta) & (41+10\beta) & (5-5\beta) & -1 & 0 & \cdots & \cdots & 0 \\ -1 & (6-5\beta) & (38+10\beta) & (6-5\beta) & -1 & 0 & \cdots & 0 \\ 0 & -1 & (6-5\beta) & (38+10\beta) & (6-5\beta) & -1 & \cdots & 0 \\ & & & & \vdots & & \vdots & \\ 0 & 0 & \cdots & -1 & (5-5\beta) & (41+10\beta) & & (3-5\beta) \\ 0 & 0 & \cdots & 0 & 0 & 0 & & 1 \end{bmatrix} \theta^2$$

$$=\begin{bmatrix} 1 & 0 & 0 & \cdots & 0 & 0 & \cdots & 0 \\ (3+8\beta) & (-16\beta+41) & (8\beta+5) & -1 & 0 & 0 & \cdots & 0 \\ -1 & (6+8\beta) & (38-16\beta) & (6+8\beta) & -1 & 0 & \cdots & 0 \\ 0 & -1 & (6+8\beta) & (38-16\beta) & (6+8\beta) & -1 & \cdots & 0 \\ \vdots & & & & & & & \vdots \\ 0 & 0 & \cdots & -1 & (5+8\beta) & (41-16\beta) & & (3+8\beta) \\ 0 & 0 & \cdots & 0 & 0 & 0 & & 1 \end{bmatrix} \theta^1-$$

$$\beta\begin{bmatrix} 0 & 0 & 0 & 0 & \cdots & 0 \\ 1 & -2 & 1 & 0 & \cdots & 0 \\ 0 & 1 & -2 & 1 & \cdots & 0 \\ \vdots & & & & & \vdots \\ 0 & 0 & \cdots & 1 & -2 & 1 \\ 0 & 0 & \cdots & 0 & 0 & 0 \end{bmatrix} \theta^0 \tag{26}$$

where θ^j is the vector of nodal water content values at time steps $j=0, 1, 2$ of Δt increments.

Equation (26) can be simplified by assuming all interpolating parabolas within a defined nodal domain to be coincident. Thus, for interior nodal domains the appropriate integrated relations become:

$$\frac{\Delta t}{12(\Delta x)}\{-(\theta_1^0-2\theta_2^0+\theta_3^0)+8(\theta_1^1-2\theta_2^1+\theta_3^1)+$$

$$5(\theta_1^2-2\theta_2^2+\theta_3^2)\}=\frac{\Delta x}{24}\{(\theta_1^2-22\theta_2^2+\theta_3^2)-$$

$$(\theta_1^1+22\theta_2^1+\theta_3^1)\} \tag{27}$$

where the first and second set of braces represent the integrated moisture influx and integrated variation of water content, respectively, between time steps Δt and $2\Delta t$ (superscripts $j=1, 2$). For $\gamma=2(\Delta t)/(\Delta x)^2$ and appropriate integration with respect to space and time on column-end nodal domains, the global matrix system corresponding to the numerical approximations of equation (20) by equations (16) and (18) is:

$$\begin{bmatrix} 1 & 0 & 0 & 0 & \cdots & 0 \\ (1-5\gamma) & (22+10\gamma) & (1-5\gamma) & 0 & \cdots & 0 \\ 0 & (1-5\gamma) & (22+10\gamma) & (1-5\gamma) & \cdots & 0 \\ & & & & & \vdots \\ 0 & \cdots & 0 & 0 & (1-5\gamma) & (22+10\gamma) & (1-5\gamma) \\ 0 & \cdots & 0 & 0 & 0 & 0 & 1 \end{bmatrix} \theta^2$$

$$=\begin{bmatrix} 1 & 1 & 0 & 0 & 0 & 0 & \cdots & 0 \\ (1+8\gamma) & & (22-16\gamma) & (1+8\gamma) & 0 & \cdots & & 0 \\ 0 & & (1+8\gamma) & (22-16\gamma) & (1+8\gamma) & \cdots & & 0 \\ \vdots & & & & & & & \vdots \\ 0 & \cdots & 0 & 0 & 0 & (1+8\gamma) & (22-16\gamma) & (1+8\gamma) \\ 0 & & 0 & 0 & 0 & 0 & 0 & 1 \end{bmatrix} \theta^1-$$

$$\gamma\begin{bmatrix} 0 & \cdots & & & & 0 \\ 1 & -2 & 1 & 0 & \cdots & 0 \\ 0 & 1 & -2 & 1 & 0 & \cdots & 0 \\ \vdots & & & & & & \vdots \\ 0 & \cdots & & 0 & 1 & -2 & 1 \\ 0 & \cdots & & 0 & 0 & 0 & 0 \end{bmatrix} \theta^0 \tag{28}$$

where specified boundary conditions are included.

Equation (28) can be further simplified temporally by letting:

$$\frac{\partial\theta}{\partial t}=\frac{\theta^{i+1}-\theta^i}{\Delta t} \tag{29}$$

Then, combining equations (27) and (29):

$$\frac{1}{2\Delta x}[(\theta_2^2-\theta_1^2)-(\theta_1^2-\theta_0^2)+(\theta_2^1-\theta_1^1)-(\theta_1^1-\theta_0^1)]$$

$$=\frac{\Delta x}{24}[(\theta_1^2-22\theta_2^2+\theta_3^2)-(\theta_1^1+22\theta_2^1+\theta_3^1)] \tag{30}$$

which results in the modified capacitance matrix formulation[6]:

$$\hat{\mathbf{P}}\ (\text{modified})\equiv\frac{\Delta x}{24}\begin{bmatrix} 11 & 1 \\ 1 & 11 \end{bmatrix} \tag{31}$$

To determine the numerical effectiveness of solving the normalized soil–water transfer problem by the formu-

Table 1. Comparison of numerical model results at x = 0.50*

Time	Finite element method†	Nodal domain integration‡	Exact solution	Finite element error (%)	Nodal integration error (%)
0.01	0.887	0.901	0.999	11	9
0.02	0.786	0.833	0.975	19	15
0.03	0.697	0.763	0.918	24	17
0.04	0.618	0.700	0.846	27	17
0.05	0.548	0.641	0.772	29	17
0.06	0.486	0.588	0.702	28	16
0.07	0.431	0.538	0.637	32	16
0.08	0.382	0.493	0.578	34	15
0.09	0.339	0.452	0.524	35	14
0.10	0.301	0.414	0.474	36	13
0.11	0.267	0.380	0.430	38	12
0.12	0.237	0.348	0.390	39	11
0.13	0.210	0.319	0.353	40	10
0.14	0.186	0.292	0.320	42	9
0.15	0.165	0.268	0.290	43	8
0.16	0.146	0.246	0.262	44	6
0.17	0.130	0.225	0.238	46	5
0.18	0.115	0.206	0.215	47	4
0.19	0.102	0.189	0.195	48	3
0.20	0.091	0.173	0.177	49	2

* Three nodal point discretization.
† Equation (32).
‡ Simplified version of nodal integration using equation (28).

lations of equations (24), (27), and (30), a Galerkin finite element analog to equation (20) was also determined for comparison. The Galerkin finite element-matrix formulation (for a linear polynomial shape function approximation) numerically approximates the normalized problem of equation (20) within each finite element by:

$$\hat{\mathbf{S}}\begin{Bmatrix}\theta_i\\ \theta_j\end{Bmatrix}+\hat{\mathbf{P}}\begin{Bmatrix}\dot{\theta}_i\\ \dot{\theta}_j\end{Bmatrix}=\frac{1}{\Delta x}\begin{bmatrix}1 & -1\\ -1 & 1\end{bmatrix}\begin{Bmatrix}\theta_i\\ \theta_j\end{Bmatrix}+\frac{\Delta x}{6}\begin{bmatrix}2 & 1\\ 1 & 2\end{bmatrix}\begin{Bmatrix}\dot{\theta}_i\\ \dot{\theta}_j\end{Bmatrix} \tag{32}$$

where $\hat{\mathbf{S}}$ and $\hat{\mathbf{P}}$ are element stiffness and capacitance matrices and (θ_i, θ_j) and $(\dot{\theta}_i, \dot{\theta}_j)$ refer to the element nodal and dynamic nodal moisture content values for an element of length Δx.

By comparison, the modified finite element-matrix system for equation (31) is:

$$\hat{\mathbf{S}}\begin{Bmatrix}\theta_i\\ \theta_j\end{Bmatrix}+\hat{\mathbf{P}}\ (\text{modified})\begin{Bmatrix}\dot{\theta}_i\\ \dot{\theta}_j\end{Bmatrix}=\frac{1}{\Delta x}\begin{bmatrix}1 & -1\\ -1 & 1\end{bmatrix}\begin{Bmatrix}\theta_i\\ \theta_j\end{Bmatrix}+\frac{\Delta x}{24}\begin{bmatrix}11 & 1\\ 1 & 11\end{bmatrix}\begin{Bmatrix}\dot{\theta}_i\\ \dot{\theta}_j\end{Bmatrix} \tag{33}$$

Results from application of equation (11) to the problem defined by equation (20) are shown in Table 1. The matrix system of equation (28) is used to better compare numerical results to the linear approximating function results of the Galerkin approximation (linear polynomial shape function) of equations (7) and (32). The numerical approximation was based on a three nodal discretization of the one-dimensional domain in which two of the nodal points are specified as boundary conditions; thus the matrix systems reduce to a single linear equation for btoh numerical approximations. From Table 1, it is seen that for this problem the numerical approach of equation (28) provides increasingly accurate results whereas the finite element approximation progressively gives poorer approximations for the same level of spatial discretization. Additionally, the numerical approach of equation (28) produces similar approximations to those obtained by revising the Galerkin capacitance matrix in accordance with equations (7) and (33).

For further comparison, the nodal domain of equation (20) was discretized by five nodal points. Comparison of numerical solutions by the Galerkin finite element approach, equations (7) and (32); the revised finite element capacitance matrix approach, equations (7) and (33); and the numerical approximation given by equation (26) to the exact solution at $x = 0.50$ are shown in Table 2. Again, the nodal integration approach provides significant improvement over the finite element method. From Table 2, the finite element matrix system revised by equation (31) gives similar results to the model of equation (26) for time greater than 0.06. However, for the initial instability to the numerical system (due to the boundary conditions) the numerical approach of equation (26) provides better approximations.

EXTENSION TO ONE-DIMENSIONAL CONVECTION–DIFFUSION EQUATION

The second order linearized partial differential equation:

$$\frac{\partial}{\partial x}k_1\frac{\partial\theta}{\partial x}+k_2\frac{\partial\theta}{\partial x}=k_3\frac{\partial\theta}{\partial t};\quad x\in R \tag{34}$$

applies to a vertical unsaturated soil column problem where the k_i are the appropriate hydraulic parameters. Discretizing the domain into uniform nodal domains R_j in accordance with equation (8), equation (34) can be integrated spatially within each nodal domain to give:

$$k_1\frac{\partial\theta}{\partial x}\bigg|_{\Gamma_j}+\int_{R_j}k_2\frac{\partial\theta}{\partial x}dx=\int_{R_j}k_3\frac{\partial\theta}{\partial t}dx \tag{35}$$

Table 2. Comparison of numerical model results at x = 0.50*

Time	Finite element method†	Revised capacitance matrix‡	Nodal integration per (26)	Exact solution
0.01	1.041	0.989	1.023	0.999
0.02	0.970	0.941	0.956	0.975
0.03	0.881	0.876	0.887	0.918
0.04	0.796	0.807	0.812	0.846
0.05	0.718	0.739	0.741	0.772
0.06	0.637	0.674	0.674	0.702
0.07	0.583	0.614	0.613	0.637
0.08	0.525	0.558	0.557	0.578
0.09	0.474	0.508	0.506	0.524
0.10	0.427	0.461	0.460	0.474
0.11	0.385	0.419	0.418	0.430
0.12	0.347	0.381	0.379	0.390
0.13	0.312	0.346	0.345	0.353
0.14	0.282	0.314	0.313	0.320
0.15	0.254	0.285	0.284	0.290
0.16	0.229	0.259	0.258	0.262
0.17	0.206	0.235	0.235	0.238
0.18	0.186	0.214	0.213	0.215
0.19	0.167	0.194	0.194	0.195
0.20	0.151	0.176	0.176	0.177

* Five nodal point discretization.
† Equation (32).
‡ Equation (33).

Table 3. Comparison of numerical model results for a vertical column

Solution	$x=0$	$x=50$	Error	$x=100$
Exact	1	0.276	0%	0
Finite element method	1	0.429	55%	0
Integration	1	0.342	24%	0

Assuming the k_i to be constant within each nodal domain during a time step Δt, and integrating with respect to time gives:

$$\int_{\Delta t}\left(k_1\frac{\partial\theta}{\partial x}\bigg|_{\Gamma_j}\right)dt+\int_{\Delta t}\left(k_2\theta\bigg|_{\Gamma_j}\right)dt=\left(\int_{R_j}k_3\theta\,dx\right)\bigg|_{\Gamma_t} \tag{36}$$

where Γ_j and Γ_t are the spatial and temporal boundaries. For θ approximated spatially and temporally by equation (18), and assuming coincident parabolic interpolation functions within each nodal domain R_j, the resulting expression for an interior nodal point θ_1 between nodal points (θ_0, θ_2) is:

$$A_1\theta_0^2+A_2\theta_1^2+A_3\theta_2^2=B_1\theta_0^1+B_2\theta_1^1+B_3\theta_2^1+C_1\theta_0^0+C_2\theta_1^0+C_3\theta_2^0 \tag{37}$$

where

$$A_1=k_3+5k_2(\Delta t/\Delta x)-5\alpha k_1$$

$$A_2=22k_3+10\alpha k_1$$

$$A_3=k_3-5k_2(\Delta t/\Delta x)-5\alpha k_1$$

$$B_1=8\alpha k_1-8k_2(\Delta t/\Delta x)+k_3$$

$$B_2=-16\alpha k_1+22k_3$$

$$B_3=8\alpha k_1+8k_2(\Delta t/\Delta x)+k_3$$

$$C_1=-k_1\alpha+k_2(\Delta t/\Delta x)$$

$$C_2=2\alpha k_1$$

$$C_3=-k_1\alpha-k_2(\Delta t/\Delta x)$$

and where $\alpha=2(\Delta t)/(\Delta x)^2$.

Disregarding the coincident parabolic interpolation function assumption, a soil-moisture transfer mass balance would occur by averaging all possible parabolic interpolations within each R_j. Accordingly, for a typical nodal point θ_2 interior to the sequence of nodal points (θ_0, θ_1, θ_3, θ_4),

$$\theta|_{R_j(\theta_2)}=\frac{1}{16}\theta_0-\frac{5}{8}\theta_1+\frac{5}{8}\theta_3-\frac{1}{16}\theta_4 \tag{38}$$

whereby equation (38) can be appropriately combined with equation (28) to give the complete mass balance formulation.

A numerical advantage of equation (37) to a linear shape function finite element (Galerkin) formulation with a Crank–Nicolson time step advancement process was found. The two methods were compared to the exact solution of the problem

$$k_1\frac{\partial^2\theta}{\partial x^2}-k_2\frac{\partial\theta}{\partial x}=\frac{\partial\theta}{\partial t} \tag{39}$$

with conditions,

$$\theta(0,t)=\theta_0,\qquad t>0$$

$$\theta(\infty,t)=0,\qquad t>0$$

$$\theta(x,0)=0,\qquad 0\leqslant x\leqslant\infty$$

The well known solution to equation (39) is the expression:

$$\frac{\theta}{\theta_0}=\frac{1}{2}\left\{\operatorname{erfc}\left[\frac{x-k_2t}{(4k_1t)^{1/2}}\right]+\exp\left[\frac{xk_2}{k_1}\right]\operatorname{erfc}\left[\frac{x+k_2t}{(4k_1t)^{1/2}}\right]\right\} \tag{40}$$

where k_1 and k_2 are assumed constant. Equation (39) was solved for arbitrarily selected values of $k_1=2.5$, $k_2=0.0625$. A time step $\Delta t=25$ was used and equation (39) was modelled by assuming that

$$\theta(100,t)=0,\qquad 0\leqslant t\leqslant 250 \tag{41}$$

in order to obtain a finite one-dimensional domain. For comparison purposes, a two element discretization of element size equal to 50 was used. A linear shape function Galerkin approximation in accordance with equations (6) and (7) was used for comparison purposes. For a total time equal to 250, the numerical results are shown in Table 3. Comparison of both numerical methods indicates consistent approximation improvement by using a model based on equation (37).

EXTENSION TO TWO-DIMENSIONS

The two-dimensional mathematical model for horizontal soil water transport in a rectangular domain R, where water content is the state variable is given by:

$$\frac{\partial}{\partial x}\left[D(\theta)\frac{\partial\theta}{\partial x}\right]+\frac{\partial}{\partial y}\left[D(\theta)\frac{\partial\theta}{\partial y}\right]=\frac{\partial\theta}{\partial t};\ (x,y)\in R \tag{42}$$

Analogous to the one-dimensional case, the domain is discretized into n rectangular nodal domains by n nodal points as shown in Fig. 2,

$$R=\bigcup_{i=1}^{n}R_i \tag{43}$$

Application of equation (42) to each R_i gives

$$\frac{\partial}{\partial x}\left[D(\theta)\frac{\partial\theta}{\partial x}\right]+\frac{\partial}{\partial y}\left[D(\theta)\frac{\partial\theta}{\partial y}\right]=\frac{\partial\theta}{\partial t};\ (x,y)\ \varepsilon\ R_i,\ \forall_T \tag{44}$$

Integrating spatially and temporally on each R_i gives:

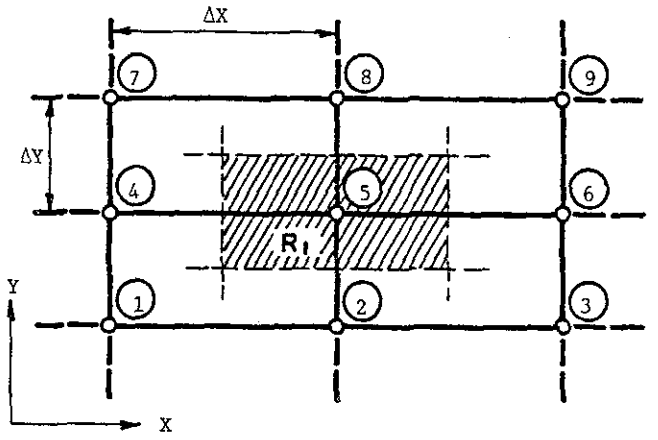

Figure 2. Two-dimensional nodal domain. (1) = *nodal point 1;* R_1 = *nodal domain number 1;* $\Delta X \sim$ *x-direction increment;* $\Delta Y \sim$ *y-direction increment;* $R = \bigcup_{i=1}^{n} R_i$

$$\int_{\Delta t}\int_{R_j}\int\frac{\partial}{\partial x}\left[D(\theta)\frac{\partial\theta}{\partial x}\right]dx\,dy\,dt+\int_{\Delta t}\int_{R_j}\int\frac{\partial}{\partial y}\left[D(\theta)\frac{\partial\theta}{\partial y}\right]dy\,dx\,dt = \int_{R_j}\int_{\Delta t}\int\frac{\partial\theta}{\partial t}dt\,dx\,dy \qquad i=1,2,..,n \tag{45}$$

or

$$\int_{\Delta t}\int_{\Delta Y}\left\{D(\theta)\frac{\partial\theta}{\partial x}\right\}_{\Gamma_x}dy\,dt+\int_{\Delta t}\int_{\Delta X}\left\{D(\theta)\frac{\partial\theta}{\partial y}\right\}_{\Gamma_y}dx\,dt = \int_{\Delta X}\int_{\Delta Y}\{\theta\}_{\Gamma_t}dx\,dy \qquad i=1,2,\ldots,n \tag{46}$$

where (ΔX, ΔY, Δt) are the spatial and temporal increments respectively and (Γ_x, Γ_y, Γ_t) are the spatial and temporal boundaries respectively. For a finite element domain discretization, assuming soil water diffusivity constant within each finite element during a time step Δt, equation (46) can be written as:

$$\int_{\Delta t}\left(\int_{0}^{\Delta Y/2}\left\{D\frac{\partial\theta}{\partial x}\right\}_{\Gamma_x}dy+\int_{\Delta Y/2}^{\Delta Y}\left\{D\frac{\partial\theta}{\partial x}\right\}_{\Gamma_x}dy\right)dt+$$

$$\int_{\Delta t}\left(\int_{0}^{\Delta x/2}\left\{D\frac{\partial\theta}{\partial y}\right\}_{\Gamma_y}dx+\int_{\Delta x/2}^{\Delta x}\left\{D\frac{\partial\theta}{\partial y}\right\}_{\Gamma_y}dx\right)dt$$

$$=\int_{\Delta X}\int_{\Delta Y}\{\theta\}_{\Gamma_t}dy\,dx \tag{47}$$

A numerical analog can be derived by considering the normalized two-dimensional horizontal moisture transfer model similar to equations (20), (21). (22),

$$\frac{\partial^2\theta}{\partial x^2}+\frac{\partial^2\theta}{\partial y^2}=\frac{\partial\theta}{\partial t}; \qquad 0\leqslant x\leqslant 1,\ 0\leqslant y\leqslant 1 \tag{48}$$

Assume θ to be approximated spatially by parabolic interpolating functions, and temporally by a linear interpolating function. The temporal term of (46) is given numerically by considering Fig. 2; i.e.

$$\int_{\Delta X}\int_{\Delta Y}\theta\,dx\,dy=\frac{\Delta X\Delta Y}{576}(\theta_1+\theta_3+\theta_7+\theta_9+22\theta_2+22\theta_4+22\theta_6+22\theta_8+484\theta_5) \tag{49}$$

The integrated x-direction influx is:

$$\frac{\Delta Y}{24\Delta X}(\theta_1-2\theta_2+\theta_3+22\theta_4-44\theta_5+22\theta_6+\theta_7-2\theta_8+\theta_9) \tag{50}$$

Similarly, the integrated y-direction influx is:

$$\frac{\Delta X}{24\Delta Y}(\theta_1+\theta_3+\theta_7+\theta_9+22\theta_2+22\theta_8-2\theta_4-2\theta_6-44\theta_5) \tag{51}$$

Combining equations (50) and (51), the net integrated influx is, for $\Delta X=\Delta Y$:

$$\frac{1}{12}(\theta_1+10\theta_2+\theta_3+10\theta_4-44\theta_5+10\theta_6+\theta_7+10\theta_8+\theta_9) \tag{52}$$

For identical constant spatial increments, the solution of equation (46) reduces to the one-dimensional problem of equation (20) for zero y-directional influx. From Fig. 2 and equations (49) and (52), the problem simplifying assumptions are:

$$\left.\begin{aligned}&\frac{\partial\theta}{\partial y}=0\\&\Delta X=\Delta Y\\&\theta_1=\theta_4=\theta_7\\&\theta_2=\theta_5=\theta_8\\&\theta_3=\theta_6=\theta_9\end{aligned}\right\} \tag{53}$$

By substitution, the matrix system defined by equations (49) and (52) reduce to the matrix system defined by equation (30).

CONCLUSIONS

The mathematical analysis leading to numerical analogs that preserve mass balance in a horizontal soil transport problem is presented. Extensions from the one-

dimensional horizontal soil-transport model to the so-called linearized convection–diffusion equation is also presented. Comparison of numerical results to the appropriate finite element numerical solutions indicate significant improvement when utilizing the mass balanced schemes.

Extension of the one-dimensional approach to two dimensions is additionally included. Although only the rectangular domain is analysed, application of the improved model to irregular domains is accomplished by using the usual finite element matrices for non-rectangular regions, and including the mass-balanced matrix systems for the remaining rectangular regions.

ACKNOWLEDGEMENTS

This research was supported by an U.S. Army Research Office Contract No. DAAG 29–79–C 0080.

REFERENCES

1 Bruch, J. C. Jr. and Zyvoloski, G. Solution of vertical unsaturated flow of soil water, *Soil Sci.* 1974, **116**, 417
2 Desai, C. S. *Elementary Finite Element Method*, Prentice-Hall, Englewood Cliffs, 1979
3 Douglas, J. Jr., and Dupont, T. Galerkin methods for parabolic equations, *SIAM J. Numer. Anal.* 1970, **7**, 575
4 Guymon, G. L. and Luthin, J. N. A coupled heat and moisture transport model for artic soils, *Water Resour. Res.* 1974, **10**, 995
5 Hayhoe, H. M. Study of relative efficiency of finite difference Galerkin techniques for modeling soil–water transfer, *Water Resour. Res.* 1978, **14**, 97
6 Hromadka, T. V. and Guymon, G. L. Some effects of linearizing the unsaturated soil-moisture transfer diffusion model, *Water Resourc. Res.* in press
7 Newman, S. P., Feddes, R. A. and Bresler, E. Finite element analysis of two-dimensional flow in soils considering water uptake by roots: I. Theory, *Soil Sci. Soc., Am. Proc.* 1975, 39
8 Price, H. S., Cavendish, J. C. and Varga, R. S. Numerical methods of higher-order accuracy for diffusion–convection equations, *Soc. Pet. Eng.* 1968, **243**, 293
9 Yoon, Y. S. and Yeh, W. W.-G. The Galerkin method for nonlinear parabolic equations of unsteady groundwater flow, *Water Resour. Res.* 1975, **11**, 751